MAGNETIC RESONANCE IN CHEMISTRY
Magn. Reson. Chem. **36**, 627–634 (1998)

NMR spectral analysis and molecular dynamics study of 3-quinuclidinol and 3-quinuclidinyl benzilate

Sami Heikkinen,[1]* Markku Mesilaakso[2] and Erkki Rahkamaa[1]

[1] Department of Chemistry, University of Oulu, P.O. Box 333, FIN-90571 Oulu, Finland
[2] Finnish Institute for Verification of the Chemical Weapons Convention, P.O. Box 55, FIN-00014 University of Helsinki, Finland

Received 20 October 1997; revised 28 January 1998; accepted 16 February 1998

ABSTRACT: Proton chemical shifts and coupling constants of 3-quinuclidinol and 3-quinuclidinyl benzilate were determined by computer analysis. The relatively broad lines of the quinuclidine protons have their origin in numerous non-resolved transitions arising from the extensively coupled spin system of 12 nuclei. The signs of the long-range coupling constants were determined by COSY-45 and E.COSY. Vicinal coupling constants were converted into proton–proton torsion angles by applying the Altona–Haasnoot equation. Some geometrical ambiguities were revealed, which were studied by molecular dynamics calculations and simulated annealing. The torsion angles and the results from molecular dynamics calculations indicated significant flexibility of the quinuclidine part. For the sake of completeness the carbon chemical shifts of both compounds are presented. © John Wiley & Sons, Ltd.

KEYWORDS: NMR; ^{1}H NMR; ^{13}C NMR; quinuclidine; 3-quinuclidinol; 3-quinuclidinyl benzilate; long-range coupling; molecular dynamics

INTRODUCTION

Numerous biologically active compounds, including the cinchona alkaloids quinine and quinidine, have a bicyclic quinuclidine skeleton. 3-Quinuclidinyl benzilate (**1**) {3-(1-azabicyclo[2.2.2]octyl) α-hydroxy-α,α-diphenylacetate, also known as BZ or Ro-2-3308} is an anticholinergic drug of the glycolate series with high psychotoxic potential, about 50-fold that of atropine.[1–4] The psychosomimetic properties of **1** possibly are due to accessibility of the lone-pair electrons of the nitrogen.[5] The inability of the bulky side-chain to form intramolecular hydrogen bonds with nitrogen may enhance the availability of the active lone-pair electron. In addition, steric effects are important in optimizing interactions between glycolate and receptor.[6] Owing to its strong psychosomimetic effect, compound **1** has potential as a chemical warfare agent[7] and its production, use and stockpiling are prohibited by the Chemical Weapons Convention.[8] 3-Quinuclidinol (**2**) (1-azabicyclo[2.2.2]octan-3-ol) is a precursor and degradation product of **1**.

The primary objective of this work was to determine the ^{1}H spectral parameters of **1** and **2** for verification purposes.[9] The quinuclidine part also provided an excellent structure for studying the long-range H–H couplings of different coupling pathways. The coupling constants were determined by spin simulation[10], and the signs of the couplings were extracted from COSY-45 and E.COSY correlations.[11–16] In particular, the four-bond couplings revealed that the sign behavior over the bridgehead nitrogen differed from that over the bridgehead carbon. The vicinal H–H coupling constants were converted into torsion angles by applying the Altona–Haasnoot equation[17] and the torsion angles were studied with molecular dynamics calculations.[18]

To our knowledge, neither the long-range couplings nor the flexibility of the quinuclidine moiety have been thoroughly studied, although various compounds containing the quinuclidine moiety have been reported.[1–3,19–21]

The assignment of the carbon resonances of both **1** and **2** was accomplished by carrying out standard ^{13}C{^{1}H}, DEPT-135,[22] HSQC[23] and HMQC[24] experiments and HETCOR optimized for long-range couplings.[25]

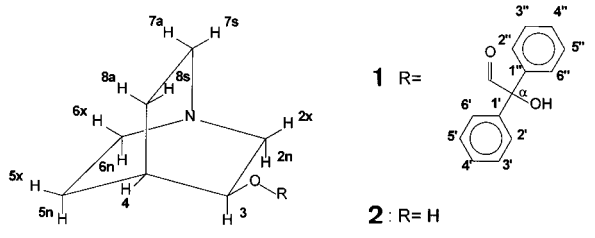

RESULTS AND DISCUSSION

The NMR spectral parameters, torsion angles of the quinuclidine part and signs of the coupling constants of **1** and **2** are presented in Table 1. The parameters obtained from analysis of the phenyl part of **1** at 600 MHz do not deviate markedly from our previous results.[26] The experimental and simulated ^{1}H spectra of

* *Correspondence to*: S. Heikkinen, Institute of Biotechnology, University of Helsinki, P.O. Box 56, FIN-00014 Helsinki, Finland.
E-mail: Tiltu@mimosa.pc.helsinki.fi
Contrant/grant sponsor: Tauno Tönning Foundation.

 CCC 0749-1581/98/090627–08 $17.50

Table 1. NMR spectral parameters [δ_H, δ_C, *vs.* $\delta_{TMS} = 0.0$ ppm; $^nJ(^1H,^1H)$, $n = 2$–5], signs of the long-range coupling constants and H—C—C—H torsion angles (Φ) for 3-quinuclidinyl benzilate (**1**) and 3-quinuclidinol (**2**), with errors in the chemical shifts and coupling constants of ± 0.1–0.2 Hz

	δ_H (ppm)				$J(^1H,^1H)$ (Hz)		$\Phi_{H,H}$ (°)			$\delta^{13}C$ (ppm)	
Nucleus	**1**	**2**	*n*	Coupled nuclei	**1**	**2**	**1**	**2**	Sign[c]	**1**	**2**
2x	2.495	2.638	2	2x, 2n	−14.68	−13.97				55.91	59.18
			3	2x, 3	2.92	3.46	−115	−119			
			4	2x, 4	0.775[a]	0.62			+		
			5	2x, 5x	[b]	[b]			−		
			4	2x, 6x	2.47	2.55			+ * W		
			4	2x, 6n	0.57	0.48					
			4	2x, 7a	0.59	0.57			+ *		
2n	3.134	3.155	3	2n, 3	8.15	8.33	10	9			
			4	2n, 6x	0.44	0.60			+ *		
			4	2n, 7s	0.58	0.58					
			4	2n, 7a	2.38	2.39			+ * W		
			5	2n, 8a	[b]	[b]			−		
3	4.918	3.911	3	3, 4	4.01	3.51	55	59		74.56	68.25
			4	3, 5n	[b]	[b]			−		
			4	3, 8s	[e]	[e]			−		
			4	3, 8a	1.45	1.36			+ W		
4	1.930	1.864	3	4, 5x	4.02	3.71	53	55		26.23	29.58
			3	4, 5n	2.74	2.81	−62	−61			
			3	4, 8s	3.58	3.37	56	57			
			3	4, 8a	2.51	2.95	−63	−60			
5x	1.625	1.759	2	5x, 5n	−13.28	−12.90				25.12	25.97
			3	5x, 6x	10.16	10.35	15	13			
			3	5x, 6n	4.54	4.93	−122	−125			
5n	1.534	1.566	3	5n, 6x	6.04	5.41	130	127			
			3	5n, 6n	10.49	10.57	15	14			
			4	5n, 8s	2.79	2.80			+ W		
6x	2.664	2.811	2	6x, 6n	−13.44	−13.30				46.96	47.32
			4	6x, 7s	0.52	0.48					
6n	2.633	2.710	4	6n, 7s	2.52	2.50					
			4	6n, 7a	0.53	0.47					
7s	2.509	2.939	2	7s, 7a	−13.37	−13.21				47.85	48.37
			3	7s, 8s	10.39	10.56	13	11			
			3	7s, 8a	6.14	5.44	130	127			
7a	2.650	2.823	3	7a, 8s	4.36	5.00	−122	−125			
			3	7a, 8a	10.67	10.60	13	14			
8s	1.441	2.088	2	8s, 8a	−12.92	−12.56				20.18	20.11
8a	1.222	1.405									
OH	2.8[f]	3.8[f]									
1′										144.17	
1″										144.23	
2′, 6′	7.466									128.28	
2″, 6″	7.473									128.26	
			4	2′, 6′[d]	2.07						
			3	2′, 3′	7.95						
			5	2′, 5′	0.58						
			4	2′, 4′	1.23						
3′, 5′	7.353									128.68	
3″, 5″	7.365									128.68	
			4	3′, 5′	1.47						
			3	3′, 4′	7.41						
4′	7.312									128.49	
4″	7.319									128.49	
α − C										81.84	
C = O										174.22	

[a] From subspectral analysis; the corresponding averaged value did not give a satisfactory match with the experimental spectrum.
[b] Very small coupling, not included in the simulation because there was no effect on the spectrum.
[c] Sign for long-range couplings. Planar W-coupling is marked with W. An asterisk denotes nitrogen as the central atom in the coupling path.
[d] Couplings in the other ring were identical
[e] −0.2 to −0.3.
[f] Approximate values.

the quinuclidine parts of **1** and **2**, together with the resonance assigments, are presented in Fig. 1 and 2.

Assignment of ^{1}H NMR spectra of quinuclidine protons

Extensively and partially strongly coupled ^{1}H NMR spectra were recorded for the quinuclidine protons of compounds **1** and **2** (Fig. 1 and 2). Although there is some overlapping of resonances, particularly in **1**, the assignments were obtained with COSY-45 by starting the analysis from proton 3. Large, four-bond couplings (W-path) make cross peaks of these interactions readily observable, allowing straightforward assignment of the *endo*- and *exo*-protons.

Signs of coupling constants

Signs of the vicinal couplings were assumed to be positive and the geminal couplings negative (Table 1). The signs of long-range couplings of **1** were determined by comparing the COSY cross peak structures with those of **2**. If peaks were not observable or were overlapped in the spectrum of **1**, the signs were assumed to be the same as in **2**. The positive couplings ^4J(3,8a) and ^4J(5n, 8s) are mediated through an approximately planar propanic W-coupling pathway. This sign behavior is in accordance with INDO-FPT calculations.[27] However, when the coupling pathway is not a planar W, as with ^4J(2x,7a), ^4J(2n,6x), ^4J(3,5n) and ^4J(3,8s), the sign of the coupling constant depends on the central atom. Coupling over four bonds, with carbon as central atom, is negative in the case of the non-W pathway. This is also in agreement with INDO-FPT calculations. However, when the central atom is nitrogen, all four-bond couplings are positive regardless of the pathway geometry. According to the orbital interactions proposed by Barfield and co-workers,[27,28] the lone-pair electrons of nitrogen interact with s-orbitals of coupled protons, mediating a coupling with a significant positive contribution. The same kind of vicinal–vicinal interaction occurs when carbon is the central atom, but the interaction of the vicinal hybrid orbital of the central carbon with a proton s-orbital does not generate such a positive contribution.

The coupling constant ^4J(2x,4) is of particular interest. On the basis of the geometrically almost similar pathways from proton 4 to protons 2n, 6x, 6n, 7s and 7a, couplings of similar magnitude and sign to ^4J(2x,4)

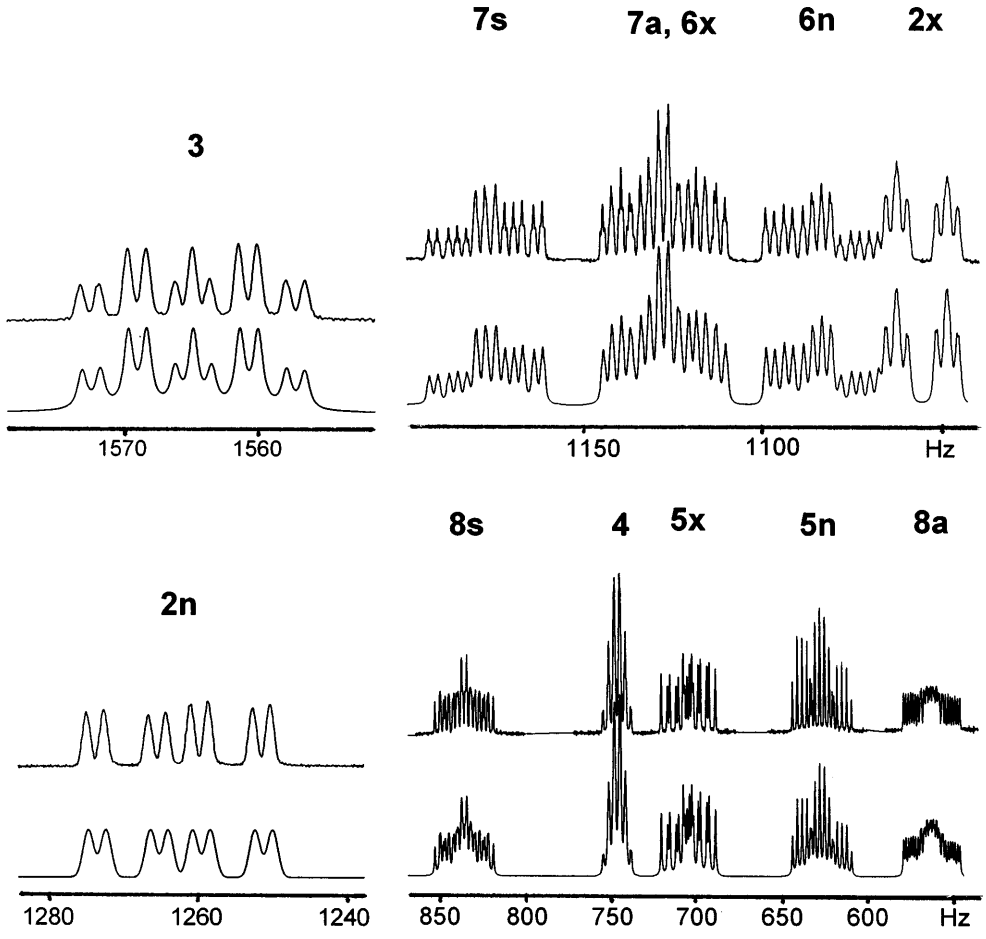

Figure 1. Expanded regions of the 400 MHz ^{1}H spectrum of 3-quinuclidinol (**2**) in acetone-d_6: comparison of the experimental (top) and simulated (bottom) resonances.

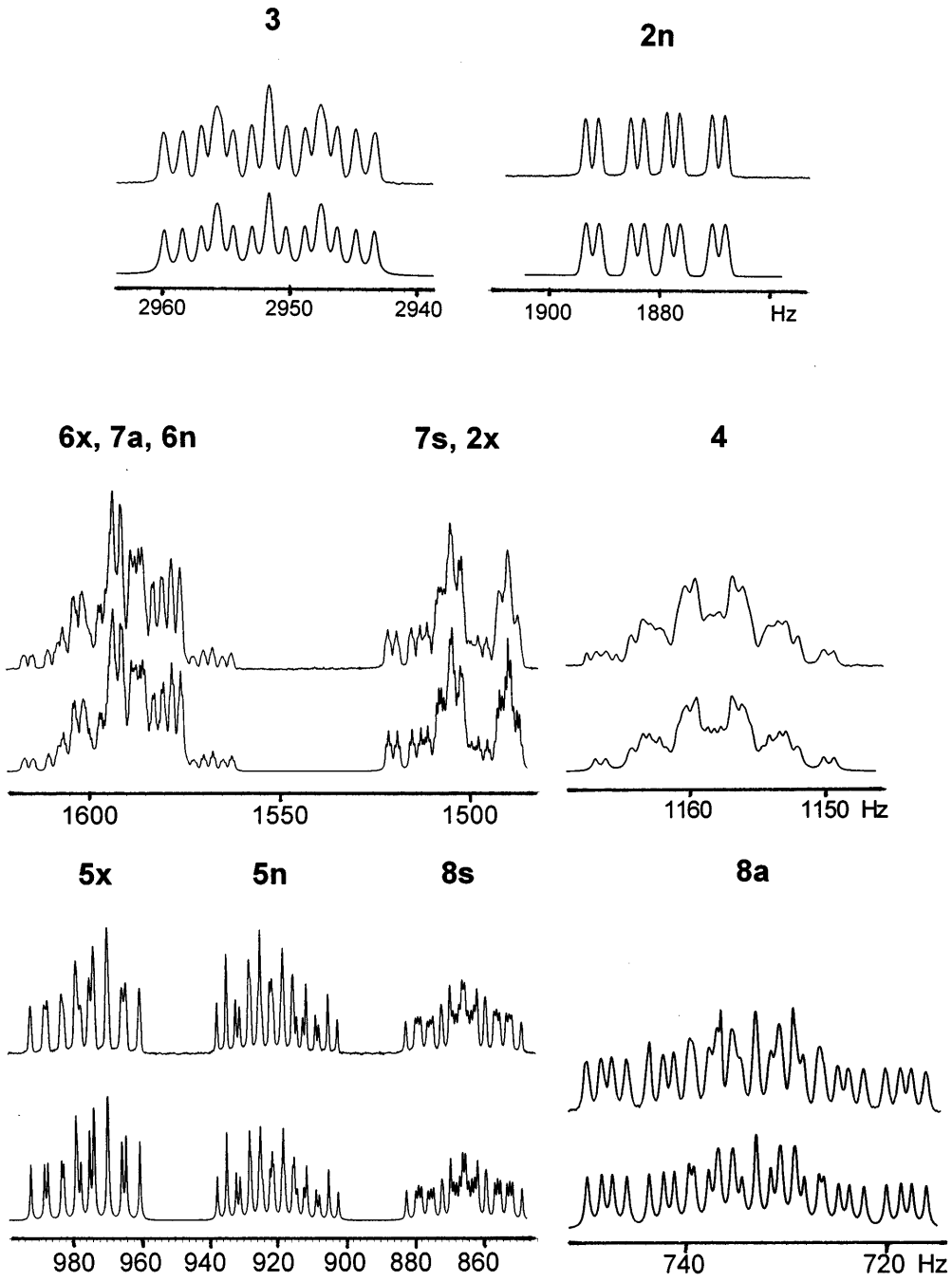

Figure 2. Expanded regions of the 600 MHz ^{1}H spectrum of the quinuclidine protons of 3-quinuclidinyl benzilate (**1**) in acetone-d_6: comparison of the experimental (top) and simulated (bottom) resonances.

would be expected, but none were observed. One explanation might be the indirect interactions between the two lone-pair electrons of oxygen and the protons 2x and 4.[27–30]

When the coupling pathway contains heteroatoms, it is difficult to decide whether the effects on $^4J(^1H,^1H)$ are due to a common substituent effect such as electronegativity, or whether they are the result of interaction between coupled protons and lone-pair electrons of the heteroatom. Interactions of lone-pair electrons of heteroatoms have been discussed by Schaefer *et al.*[30]

The signs of the couplings over five bonds [^5J(2x,5x) and ^5J(2n,8a)] are negative. Since the couplings are very small, the tilts of COSY-45 correlations are weak, and consequently the signs are considered tentative. The coupling constant ^4J(6n,7s) was assumed to be positive, analogously to ^4J(2n,7a).

Analysis of the 400 MHz ^{1}H NMR spectrum of 3-quinuclidinol (2)

The 400 MHz ^{1}H spectrum of **2** in acetone-d_6 is mainly first order. Seven subspectral analyses were performed. In most cases the spin systems constituted less than 10 spins. Regardless of observations in the COSY-45 and the long-range-COSY, a coupling was not analyzed if it was too small in magnitude to affect the 1D spectrum.

Assignment of theoretical lines was relatively simple for protons 2n, 3, 5x, 5n, 6n and 7s, because no overlapping occurred and the spectral lines were well separated (Fig. 1). The resonance of proton 2x had almost no fine structure and the resonances of 7a and 6x overlapped. Iteration of ^3J(4,5x) from the resonance of 5x gave 3.71 Hz, whereas iteration from the resonance of 4 yielded 3.50 Hz. Similarily, iteration of ^3J(4,8s) from the resonances of 8s and 4 gave 3.06 and 3.48 Hz, respectively. For the determination of the correct value (3.37 Hz, Table 1), ^3J(4,5x) was fixed at 3.71 Hz and the multiplet of proton 4 was used to iterate ^3J(4,8s). The multiplet of the proton 8s contained information from ^3J(4,8s) in lines with almost no fine structure. Iteration gave too small a value if the assignments were placed to the center of the broad lines. Closer inspection of these lines revealed fine structure which enabled peak-top-fitting iteration of ^4J(3,8s) and ^3J(4,8s). Table 1 presents the averaged NMR parameters of subspectral analyses and Fig. 1 the corresponding theoretical spectrum. The analysis was further confirmed with phase-sensitive DQF-COSY.[31] The results of computer analysis were in good agreement with the PS-DQF-COSY, where the largest deviations were detected for couplings from 0.2 to 0.9 Hz as a result of antiphase cancellation.[32] Also, the F_2 resolution of the 2D experiment (0.2 Hz per point) limited the accuracy.

Analysis of the 600 MHz ^{1}H NMR spectrum of quinuclidine protons of 3-quinuclidinyl Benzilate (1)

A major problem with the analysis of the ^{1}H NMR spectrum of **1** in acetone-d_6 is the serious overlap of resonances of protons 6x, 7a and 6n and the moderate overlap of resonances of protons 7s and 2x. The simulation program allowed the simultaneous analysis of these overlapping signals. Eight subspectral analyses were performed. Averaged NMR parameters are shown in Table 1.

The correctness of the averaged NMR parameters was tested by simulating the 12-spin system of the quinuclidine part as a whole (Fig. 2). In addition, the data were checked with PS-DQF-COSY and E.COSY and with the analysis of a 600 MHz ^{1}H spectrum in benzene-d_6. The coupling constants (Table 1) were in agreement with the 2D NMR results and with the study in benzene-d_6.

Broad spectral lines

The ^{1}H NMR spectral lines of the quinuclidine protons of both **1** and **2** are broader (linewidth = 0.5–0.7 Hz) than expected on the basis of their molecular weights. This is not due to poor resolution (TMS linewidth = 0.19 Hz). The resonance lines of the phenyl protons of **1** were narrow (0.23 Hz).

To investigate the reason for broad lines, we recorded the 28.9 MHz ^{14}N NMR spectra of **1** and **2**. The linewidth at half-height for the ^{14}N resonance of **1** was 4900 Hz, whereas for **2** it was 720 Hz (line broadening factor = 100 Hz for **2**). Assuming $T_1 = T_2$ for quinuclidine nitrogens, the self-decoupling[33] is less effective in the case of **2**, and the ^{1}H spectrum of **2** more sensitively expresses the possible residual broadening due to $^2J(^{14}\text{N},^1\text{H})$.

The 400 MHz $^1\text{H}\{^{14}\text{N}\}$ spectra of both **1** and **2** were recorded to determine whether there is residual broadening due to $^2J(^{14}\text{N},^1\text{H})$ in the resonances of 2x, 2n, 6x, 6n, 7s and 7a. However, no line narrowing could be observed. It is concluded that the observed linewidth is mainly due to many close and non-resolved transitions arising from an extensively J-coupled spin system.

Dynamic processes could be considered as a source of the line broadening. Molecular dynamics calculations confirmed the lifetimes of the right- and left-handed twisted conformations to be 600 fs. Hence the twisting of the quinuclidine skeleton is too fast even at 210 K to allow separation of resonances arising from the different conformations of **1**.

Proton–proton torsion angles and molecular dynamics

Torsions in the C(5)H_2—(C(6)H_2 and C(7)H_2—(C(8)H_2 fragments revealed some geometric discrepancies. The signs of torsion angles are defined according to Altona and co-workers.[17] The clockwise torsion angle is defined as positive and anticlockwise angle as negative. Correspondingly, the right-handed twist of the quinuclidine structure is characterized by positive torsion angles for *exo–exo*, *endo–endo*, *anti–anti* and *syn–syn* protons. If the torsion angle $\Phi_{5x,6x} = 13°$ and $\Phi_{5n,6n} = 14°$ in **2**, the torsions $\Phi_{5x,6n} = -125°$ and $\Phi_{5n,6x} = 127°$ are structurally impossible (Table 1). The anomaly is thought to arise from interconversion of the structure between two extremes, right-handed twist ($\Phi_{7s,8s} \approx 15°$) and left-handed twist ($\Phi_{7s,8s} \approx -15°$) and consequent averaging of coupling constants, rather than from inaccuracy of the Altona–Haasnoot equation.[17] This was studied by molecular dynamics and simulated annealing, followed by minimization of the structures. Both the molecular dynamics and the simulated annealing confirmed the right- and left-handed twisted structures. The energy barrier for twisting was *ca.* 0.4 kcal mol^{-1} (1 kcal = 4.184 kJ) and was determined by constraining the torsion angle $\Phi_{7s,8s}$ to a desired value. The low barrier for twisting and the molecular dynamics results clearly confirm the flexibility of the quinuclidine skeleton at 303 K, and consequently the observed $^3J(^1\text{H},^1\text{H})$ values and the calculated $\Phi_{\text{H,H}}$ data are all averaged values.

The situation is different with **1** because of the bulky side-chain. Quinuclidine structures generated by simulated annealing from both the right- and left-handed

twists were divided into two subsets according to different side-chain positions. After minimizing the structures, two of them with different side-chain positions were selected for molecular dynamics study at 298 K. Torsions C(2)—C(3)—O—CO were −94 to −40° and −186 to −149°, but no interconversion from one region to another appeared.

However, when molecular dynamics calculations[18] were performed using Gasteiger–Hückel charges, and the dielectric constant of acetone (20.7) was applied, the side-chain position also changed. The energy barrier for rotation about the C(3)—O bond was calculated by constraining the torsion C(2)—C(3)—O—CO from −180 to 180° in steps of 2° [Fig. 3(A)]. The energy barrier, about 5 kcal mol^{-1}, is rather small and allows interconversion of the structures between the two torsion regions. By way of comparison, the Sybyl program predicted a barrier of 4.5 kcal mol^{-1} for rotation in ethane.

As a conclusion, at the temperature of the ^1H NMR measurement, a sufficient amount of energy is available to induce averaging between the two side-chain positions of **1** and twisting of the quinuclidine skeleton between the left- and right-handed structures. Potential energy curves for twisting of the quinuclidine skeleton in **1** and **2** are presented in Fig. 3(B) and 3(C), respectively. In **2**, twisting of the bicyclic structure can be seen in the occurrence of almost equal absolute values of torsions $\Phi_{5x,6n}$ and $\Phi_{5n,6x}$. For **1** the absolute value of $\Phi_{5x,6n}$ is 8° smaller than $\Phi_{5n,6x}$; and similarily $\Phi_{7a,8s}$ is smaller than $\Phi_{7s,8a}$.

In principle, the torsion angle anomalies could be explained by the inaccuracy of the Altona–Haasnoot equation (5–10°) and by assuming that there is just one quinuclidine ring conformation for compounds **1** and **2**. However, the vicinal coupling constants and resulting torsion angles across C(5)—C(6) and C(7)—C(8) bridges are too similar to be just a result of equation inaccuracy and it is more likely that the observed discrepancies arise from fluctuation of the quinuclidine skeleton.

As the force field used is very empirical, the values of the energy minima in Fig. 3(B) and (C) cannot be used to estimate the relative conformer populations of right- or left-handed structures. Instead, it is sufficient to note the low energy barrier for fluctuation between the two extremes. Again, the barrier height is only qualitative and shoud be compared with that calculated for ethane rotation. To estimate the relative conformer populations of right- and left-hand structures, model structures (right- and left-hand twisted) for both compounds **1** and **2** were calculated.[18] The proton–proton torsion angles of the models were converted into $^3J(^1H,^1H)$ values using the Altona–Haasnoot equation and conformer populations were iterated to achieve best fit between the calculated equilibrium $^3J(^1H,^1H)$ data and the experimental values. Based on these rather crude model structures, we conclude that the conformer populations of the right-hand twisted structures seem to be slightly larger than the populations for left-hand twisted structures for both **1** and **2**. The population difference is slightly smaller for **2**. The early x-ray results obtained from quinuclidinyl benzilate hydrobromide confirm the right-handed twist of quinuclidine ring in solid state.[4b]

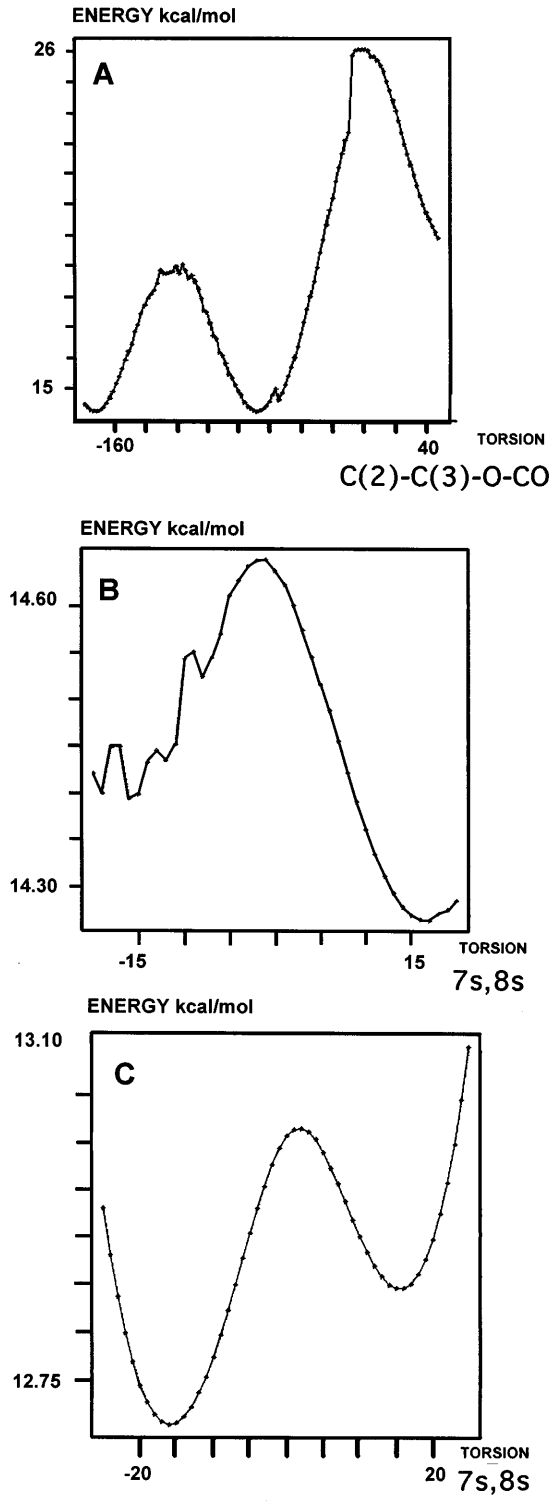

Figure 3. (A) Potential energy curves for the sidechain rotation about the C(3)—O bond in 3-quinuclidinyl benzilate (**1**), (B) twisting of the quinuclidine skeleton in **1**, and (C) corresponding twisting in **2**.

EXPERIMENTAL

The NMR experiments were performed on Bruker AMX-600, AMX-400, DPX-400, DRX-500 and Varian

Unity Plus 500 spectrometers. The NMR samples were prepared by dissolving 3 mg of 3-quinuclidinyl benzilate (synthesized in the laboratory of the Defence Forces of Finland) in 0.9 ml of acetone-d_6 (Fluka, 99.95% D) and 5 mg of 3-quinuclidinol (Sigma) in 0.8 ml of acetone-d_6 (Fluka, 99.95% D). Tetramethylsilane (TMS) served as chemical shift reference ($\delta_H = \delta_C = 0.0$ ppm). Both samples were filtered and degassed using the freeze–pump–thaw method. The 5 mm o.d. NMR tubes were sealed with a flame under reduced pressure.

The 600 MHz ^{1}H spectrum of 3-quinuclidinyl benzilate was recorded at 298 K with 32 scans, a 5263.2 Hz spectral width, 128K points in the time domain, a 12.45 s acquisition time, a 30 ms relaxation delay and a 8.5 μs pulse width. The FID was zero-filled to 512K and multiplied by a Lorentz–Gauss window (LB = −0.35 and GB = 0.2).

The 400 MHz ^{1}H spectrum of 3-quinuclidinol was recorded at 303 K with eight scans, a 1201.9 Hz spectral width, 32K points in the time domain, a 13.63 s acquisition time, a 5.0 s relaxation delay and a 12.4 μs pulse width. The FID was multiplied by a Lorentz–Gauss window (LB = −0.25 and GB = 0.2).

The 500 MHz phase-sensitive, double-quantum filtered COSY of 3-quinuclidinyl benzilate was recorded with a 2495 Hz spectral width in both dimensions. The number of points was 8K (t_2) and 2K (t_1) in raw data and 4K (F_2) and 2K (F_1) in Fourier transformed data. A shifted sine square window function was used in both dimensions. The 500 MHz E.COSY spectrum was recorded with a 1200 Hz spectral width in both dimensions. The number of points was 4K (t_2) and 512 (t_1) in raw data and 8K (F_2) and 2K (F_1) in Fourier transformed data. A shifted sine square window function was applied in the t_2 dimension and a shifted sine/Gaussian window in the t_1 dimension.

The 500 MHz phase-sensitive, double-quantum filtered COSY of 3-quinuclidinol was recorded with a 1746 Hz spectral width in both dimensions. The number of points was 8K (t_2) and 2K (t_1) in raw data and 8K (F_2) and 2K (F_1) in Fourier transformed data. A shifted sine square window function was used in both dimensions.

The 28.9 MHz ^{14}N spectra were recorded at 300 K using a 10 mm broadband probehead and 5 mm o.d. NMR tubes. The number of scans was 32K for 3-quinuclidinol and 64K for 3-quinuclidinyl benzilate and the spectral widths were 116.27 and 20.20 kHz, respectively. Acquisition times were 0.20 s and 0.11 s, relaxation delays were set to 3 μs and the pulse widths were 19 and 24.5 μs. The number of points was 46 509 for 3-quinuclidinol and the FID was zero-filled to 128K prior to Fourier transformation. Exponential weighting (LB = 100 Hz) was applied. For 3-quinuclidinyl benzilate, the number of spectral points was 4358 and the FID was zero-filled up to 16K prior to Fourier transformation. Exponential weighting (LB = 30 Hz) was applied.

The 400 MHz ^{1}H$\{^{14}$N$\}$ spectra were recorded at 300 K using a 10 mm broadband probehead and 5 mm o.d. samples. The ^{14}N decoupling experiments were performed using the MLEV decoupling sequence[34] with 6 and 12 dB attenuation. The relaxation delay was set to 1 s.

Spectral analysis was carried out using the MLDC-iterator of PERCH-software.[10] MLDC allows conventional LAOCOON3-type analysis,[35,36] peak-top fitting,[37,38] which eliminates errors in transition positions of small splittings due to linewidth, and integral-transform fitting.[39–41] Subspectral analysis was carried out because of limitation in the maximum number of spins ($\leqslant$10).

The subspectral analyses of **2** were mainly performed with the LAOCOON3 option, and in one case peak-top fitting and in one case integral-transform fitting were applied. For **1**, the resonances of protons 6x, 7a and 6n were particularly difficult to analyze with the LAOCOON3 option owing to overlapping lines. Therefore, an integral-transform fitting was carried out and the spectral parameters were refined by LAOCOON3-type analysis. Three of the subspectra were analyzed only by integral-transform fitting. The results for both **1** and **2** were checked using the latest version of the PER-iterator of PERCH software.[10] Larger spin systems can be calculated with this iterator. The error in the coupling constants is approximately ±0.1–0.2 Hz.

Energy minimization, molecular dynamics study and simulated annealing calculations were performed with Sybyl 6.1[18] on a Silicon Graphics Iris 4D/320GTX workstation. The calculations were done using a Tripos forcefield[18] with and without Gasteiger–Hückel charges and the dielectric constant of acetone (20.7). Termination of minimization occurred when the root mean square of the gradient of the energy was less than 0.05 kcal mol^{-1} Å^{-1} (0.005 kcal mol^{-1} Å^{-1} to calculate right- and left-handed model structures). Simulated annealing calculations were performed 10 times by keeping the molecule at 700 K for 1000 fs and cooling to 200 K during 1000 fs. The final structures obtained from the annealing cycles were minimized. The molecular dynamics calculations were done using a canonical ensemble, a 1000–10 000 fs simulation time and the temperature of the corresponding ^{1}H NMR measurement.

Acknowledgements

Financial support to S.H. from the Tauno Tönning Foundation is gratefully acknowledged. Special thanks are extented to the staff of the instrument manufacturers' laboratories: Peter Sandor (Varian), Detlef Moskau (Bruker Spectrospin), Naoyuki Fujii (Jeol) and Thomas Klason (Bruker Spectrospin).

REFERENCES

1. H. J. Wadsworth, S. M. Jenkins, B. S. Orlek, F. Cassidy, M. S. G. Clark, F. Brown, G.J. Riley, D. Graves, J. Hawkins and C. B. Naylor, *J. Med. Chem.* **35**, 1280 (1992).
2. V. I. Cohen, R. E. Gibson, L. H. Fan, R. De La Cruz, M. S. Gitler, E. Hariman and R. C. Reba, *J. Med. Chem.* **34**, 2989 (1991).
3. V. H. Audia, D. W. McPherson, M. Weitzberg, W. J. Rzeszotarski, B. Sturm, J. F. Kachur, M. Abreu and C. Kaiser, *J. Med. Chem.* **33**, 307 (1990).

4. (a) A. Meyerhöffer, *The Molecular Structure of Some Anticholinergic Drugs*, FOA Reports, Vol. 6, No. 13, FOA 1 Rapport B 1242-C 2, pp. 1–25. FOA, Stockholm (1972); (b) A. Meyerhöffer and D. Carlström, *Acta Crystallogr., Sect. B* **25**, 1119 (1969).
5. J. Baumgold, L. G. Abood and W. P. Hoss, *Life Sci.* **17**, 603 (1975).
6. L. G. Abood, *Handbook of Experimental Pharmacology III*, pp. 331–347. Springer, Berlin (1982).
7. S. Franke, *Lehrbuch der Militärchemie*, Band I, pp. 202–214. Deutscher Miltärverlag, Berlin (1977).
8. *Convention on the Prohibition of the Development, Production, Stockpiling and Use of Chemical Weapons and on their Destruction*, signed in January 1993, printed and distributed by the Provisional Technical Secretariat of the Preparatory Commission for the Organisation for the Prohibition of Chemical Weapons (1993). The Depositary of this Convention is the Secretary-General of the United Nations, from whom a certified true copy can be obtained.
9. E. 1. Computer-Aided Techniques for the Verification of Chemical Disarmament. E. Verification Database, in *Methodology and Instrumentation for Sampling and Analysis in the Verification of Chemical Disarmament*, edited by M. Rautio. Ministry of Foreign Affairs of Finland, Helsinki (1988).
10. R. Laatikainen, U. Weber and M. Niemitz, *PERCH—An Integrated Software for Analysis of NMR Spectra on PC*, PERCH Project, University of Kuopio, Kuopio (1994–1996).
11. C. Griesinger, O. W. Sörensen and R. R. Ernst, *J. Am. Chem. Soc.* **107**, 6394 (1985).
12. C. Griesinger, O. W. Sörensen and R. R. Ernst, *J. Chem. Phys.* **85**, 6837 (1986).
13. C. Griesinger, O. W. Sörensen and R. R. Ernst, *J. Magn. Reson.* **75**, 474 (1987).
14. R. R. Ernst, G. Bodenhausen and A. Wokaun, *Principles of Nuclear Magnetic Resonance in One and Two Dimensions*, 5th ed., pp. 414–422. Oxford Science Publications, Oxford (1992).
15. A. Bax and R. Freeman, *J. Magn. Reson.* **44**, 542 (1981).
16. A. Bax, *Two Dimensional Nuclear Magnetic Resonance in Liquids*, pp. 69–84. Delft University Press, Delft (1982).
17. (a) C. A. G. Haasnoot, F. A. A. M. de Leeuw and C. Altona, *Tetrahedron* **36**, 2783 (1980); (b) C. Altona, R. Francke, R. de Haan, J. H. Ippel, G. J. Daalmans, A. J. A. Westra Hoekzema and J. v. Wijk, *Magn. Reson. Chem.* **32**, 670 (1994).
18. *SYBYL, Molecular Modelling Software, Ver. 6.1.*, TRIPOS (1994).
19. G. D. H. Dijkstra, R. M. Kellogg, H. Wynberg, J. S. Svendsen, I. Marko and K. B. Sharpless, *J. Am. Chem. Soc.* **111**, 8069 (1989).
20. G. D. H. Dijkstra, R. M. Kellogg and H. Wynberg, *J. Org. Chem.* **55**, 6121 (1990).
21. R. J. Snow, R. Baker, R. H. Herbert, I. J. Hunt, K. J. Merchant and J. Saunders, *J. Chem. Soc., Perkin Trans. 1* 409 (1991).
22. M. R. Bendall, D. T. Doddrell and D. T. Pegg, *J. Am. Chem. Soc.* **103**, 4603 (1981).
23. G. Bodenhausen and D. Ruben, *J. Chem. Phys. Lett.* **69**, 185 (1980).
24. A. Bax, R. H. Griffey and B. L. Hawkins, *J. Magn. Reson.* **55**, 301 (1983).
25. A. Bax, and G. A. Morris, *J. Magn. Reson.* **42**, 501 (1981).
26. E. Rahkamaa and M. Mesilaakso, in *D.2. Standard Operating Procedures for the Verification of Chemical Disarmament. D. Second Proposal for Procedures Supporting the Reference Database*, pp. 235–250, 323–406 edited by M. Rautio. Ministry of Foreign Affairs of Finland, Helsinki (1989).
27. M. Barfield, A. M. Dean, C. J. Fallick, R. J. Spear, S. Sternhell and P. W. Westerman, *J. Am. Chem. Soc.* **97**, 1482 (1975).
28. M. Barfield and B. Chakrabarti, *Chem Rev.* **69**, 757 (1969).
29. M. Barfield, *J. Am. Chem. Soc.* **93**, 1066 (1971).
30. T. Schaefer, J. P. Kunkel, W. Schurko and G. M. Bernard, *Can. J. Chem.* **72**, 1722 (1994).
31. U. Piantini, O. W. Sörensen and R. R. Ernst, *J. Am. Chem. Soc.* **104**, 6800 (1982).
32. D. E. Wemmer, *Concepts Magn. Reson.* **1**, 59 (1989).
33. R. K. Harris, *Nuclear Magnetic Resonance Spectroscopy*, 2nd ed., pp. 139–141. Longman, Harlow (1986).
34. M. H. Levitt, *J. Magn. Reson.* **47**, 328 (1982).
35. S. Castellano and A. A. Bothner-By, *J. Chem. Phys.* **41**, 3863 (1964).
36. S. Castellano and A. A. Bothner-By, *LAOCN3, QCPE 111.*
37. R. Laatikainen, *Magn. Reson. Chem.* **24**, 588 (1986).
38. R. Laatikainen, *J. Magn. Reson.* **78**, 127 (1988).
39. P. Diehl, S. Sykora and J. Vogt, *J. Magn. Reson.* **19**, 67 (1975).
40. R. Laatikainen, *J. Magn. Reson.* **92**, 1 (1991).
41. R. Laatikainen, M. Niemitz, U. Weber, J. Sundelin, T. Hassinen and J. Vepsäläinen, *J. Magn. Reson. A* **120**, 1 (1996).

